

Neuropilin-1 mediates neutrophil elastase uptake and cross-presentation in breast cancer cells

Received for publication, January 3, 2017, and in revised form, April 24, 2017 Published, Papers in Press, May 3, 2017, DOI 10.1074/jbc.M116.773051

 Celine Kerros, Satyendra C. Tripathi, Dongxing Zha, Jennifer M. Mehrens, Anna Sergeeva, Anne V. Philips, Na Qiao, Haley L. Peters, Hiroyuki Katayama, Pariya Sukhumalchandra, Kathryn E. Ruusaard, Alexander A. Perakis, Lisa S. St. John, Sijie Lu,  Elizabeth A. Mittendorf,  Karen Clise-Dwyer, Amanda C. Herrmann, Gheath Alatrash, Carlo Toniatti,  Samir M. Hanash, Qing Ma, and Jeffrey J. Molldrem¹

From the University of Texas M. D. Anderson Cancer Center, Houston, Texas 77030

Edited by Alex Tokor

Neutrophil elastase (NE) can be rapidly taken up by tumor cells that lack endogenous NE expression, including breast cancer, which results in cross-presentation of PR1, an NE-derived HLA-A2-restricted peptide that is an immunotherapy target in hematological and solid tumor malignancies. The mechanism of NE uptake, however, remains unknown. Using the mass spectrometry-based approach, we identify neuropilin-1 (NRP1) as a NE receptor that mediates uptake and PR1 cross-presentation in breast cancer cells. We demonstrated that soluble NE is a specific, high-affinity ligand for NRP1 with a calculated K_d of 38.7 nM. Furthermore, we showed that NRP1 binds to the RRXR motif in NE. Notably, NRP1 knockdown with interfering RNA or CRISPR-cas9 system and blocking using anti-NRP1 antibody decreased NE uptake and, subsequently, susceptibility to lysis by PR1-specific cytotoxic T cells. Expression of NRP1 in NRP1-deficient cells was sufficient to induce NE uptake. Altogether, because NRP1 is broadly expressed in tumors, our findings suggest a role for this receptor in immunotherapy strategies that target cross-presented antigens.

Neutrophil elastase (NE)² is a serine protease stored in the azurophilic granules of neutrophils. NE plays a major role in host defense mechanisms and coordinates innate immune responses (1). NE also plays a key role in physiologic inflammation, as well as cancer metastasis and cell proliferation (2–7).

This work was supported by the Leukemia and Lymphoma Society Translational Research Program Grant (6030-12), National Institutes of Health (NIH) SPORE (P50 CA100632), Research Program Project (P01 CA049639 and P01 CA148600) grants (to J. J. M.), NIH Training Program in Cancer Immunobiology T32 CA009598 (to H. L. P. and C. K.), and National Cancer Institute Grant P30CA16672 (to the South Campus Flow Cytometry & Cell Sorting Core Facility and the Characterized Cell Line Core Facility at MDACC). The authors declare that they have no conflicts of interest with the contents of this article. The content is solely the responsibility of the authors and does not necessarily represent the official views of the National Institutes of Health.

This article contains supplemental Methods and Figs. S1–S4.

¹ To whom correspondence should be addressed: Section of Transplantation Immunology, Dept. of Stem Cell Transplantation and Cellular Therapy, Unit 900, University of Texas M. D. Anderson Cancer Center, 1515 Holcombe Blvd., Houston, TX 77030. Tel.: 713-563-3334; Fax: 713-563-3364; E-mail: jmolldre@mdanderson.org.

² The abbreviations used are: NE, neutrophil elastase; BrCa, breast cancer; CPZ, chlorpromazine; CRISPR, clustered regularly interspaced short palindromic repeats; CTL, cytotoxic T cell; HLA-A2, human leukocyte antigen-A2; NRP1, neuropilin-1; OVA, ovalbumin; MDACC, M. D. Anderson Cancer Center; PDB, Protein Data Bank; MFI, median fluorescence intensity.

Moreover, NE expression can predict the responses of trastuzumab, a monoclonal antibody that targets HER2, in metastatic breast cancer (8) and could be a prognostic marker (9). A number of studies have shown that NE is taken up by a variety of malignancies that lack endogenous NE expression (2, 10–12). Houghton and co-workers (2, 13) demonstrated that NE uptake promotes lung cancer cell proliferation by degrading insulin receptor substrate-1 and activating PI3K. We demonstrated that solid tumors, including melanoma and breast cancer, take up exogenous soluble and neutrophil-derived NE (10, 12). In addition, we have shown that PR1, an HLA-A2-restricted peptide derived from NE and proteinase 3, was cross-presented on HLA-A2 breast cancer (BrCa) cells after co-culture with NE or proteinase 3 (10). PR1 is a well defined peptide that has been targeted clinically with a PR1-peptide vaccine (14–16) and preclinically with an anti-PR1/HLA-A2 monoclonal antibody (8F4) and cellular therapies (17–19). Importantly, we have shown that PR1 cross-presentation on BrCa increased the susceptibility of the cells to lysis by PR1-specific cytotoxic T cells (CTLs) and 8F4 mAb (18).

Critically, we showed that NE uptake was dose- and time-dependent and was saturable in BrCa, which strongly suggests a receptor-mediated mechanism of uptake (12). NE was partially localized to an early endosome compartment 10 min after uptake, which further supports the presence of a receptor. Furthermore, Gregory *et al.* (2) provided evidence that NE binds to the surface of tumor cells and is internalized via clathrin-pit-mediated endocytosis. In that study, radioligand-binding experiments showed that NE binds to the surface of lung cancer cells and displayed a dissociation constant (K_d) of 284 nM, implicating the presence of a low affinity surface receptor for NE. Other investigators have also suggested the presence of an NE receptor, but to date no receptor has been identified (20, 21). Based on this knowledge, and on our previous work demonstrating that NE is taken up by a variety of tumor types (10), we hypothesized that an NE receptor is expressed in different solid tumors and mediates uptake. Identification and characterization of the receptor could lead to a better understanding of tumor mechanisms of antigen cross-presentation and proliferation and, broadly, to the interactions of the innate and adaptive immune responses.

In the current study, we confirmed that NE is taken up via a receptor-mediated mechanism in solid tumor cells. Herein, using a combination of immunoprecipitation and MS techniques, we found neuropilin-1 (NRP1), a protein overexpressed

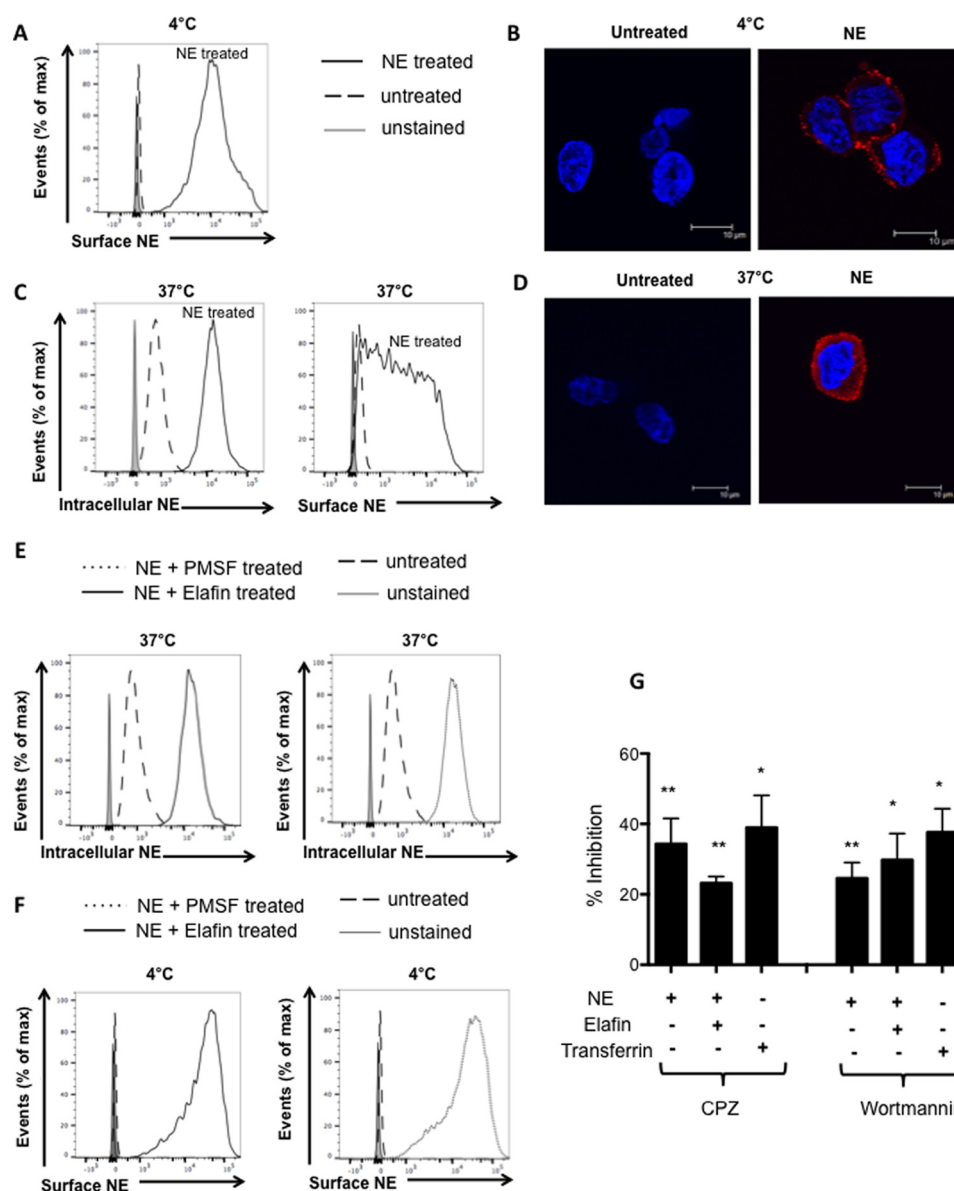


Figure 1. Surface binding and internalization of NE by MDA-MB-231 cells. A–D, MDA-MB-231 cells were incubated with soluble NE (10 μ g/ml) for 10 min at 4 $^{\circ}$ C (A and B) and 37 $^{\circ}$ C (C and D). Cell surface and intracellular NE were determined by flow cytometry (A and C) and confocal microscopy (B and D) using the anti-NE Ab conjugated to Alexa 647. Representative histogram and image from three independent experiments were shown. E–G, NE uptake is enzyme-independent and clathrin- and PI3K-dependent. MDA-MB-231 cells were incubated with soluble NE (10 μ g/ml) \pm elafin (10 μ g/ml) or PMSF (0.1 mM) for 10 min at 4 $^{\circ}$ C (E) and 37 $^{\circ}$ C (F). Intracellular (E) and cell surface (F) NE were determined by flow cytometry. G, MDA-MB-231 cells were pulsed for 10 min with NE (10 μ g/ml) \pm elafin (10 μ g/ml) after a preincubation with wortmannin or CPZ, presented as a percentage of inhibition = $[1 - (\text{MFI of cells treated with inhibitors and ligand}/\text{MFI of cells treated with ligand})] \times 100$. **, $p < 0.01$; *, $p < 0.05$ (F). Representative histograms and images from at least three independent experiments are shown.

by solid tumors (22), as the receptor for NE on the surface of MDA-MB-231 BrCa cells. We also showed that NE binds to NRP1 via its RRAR motif. NRP1 mediates NE uptake and subsequent cross-presentation of PR1, which is required for the specific lysis of MDA-MB-231 cells by PR1-CTL. Altogether, our data demonstrate a novel mechanism for NE uptake, which could lead to a better understanding of antigen cross-presentation by solid tumors and potential implications in immunotherapy.

Results

Identification of NRP1 as a cell surface receptor for NE

Using the triple-negative (ER[−]/PR[−]/HER2[−]) breast cancer cell line MDA-MB-231, which does not express NE (8), we first

assessed the ability of NE to bind to the cell surface. After incubating cells with soluble NE at 10 μ g/ml for 10 min at 4 $^{\circ}$ C, we detected NE surface staining on MDA-MB-231 cells by FACS (Fig. 1A) and confocal microscopy (Fig. 1B). Furthermore, we found both intracellular and surface staining of NE when soluble NE was incubated with MDA-MB-231 cells at 37 $^{\circ}$ C (Fig. 1, C and D). To determine whether the catalytic activity of NE is required for its short-term uptake, we preincubated NE with elafin (6 kDa), a small endogenous reversible inhibitor of NE enzymatic activity, and PMSF, a nonspecific and irreversible serine protease inhibitor. The efficiency of the protease inhibitors was assessed using EnzChek enzyme assays and presented as supplemental Fig. S1 and supplemental Methods. As shown

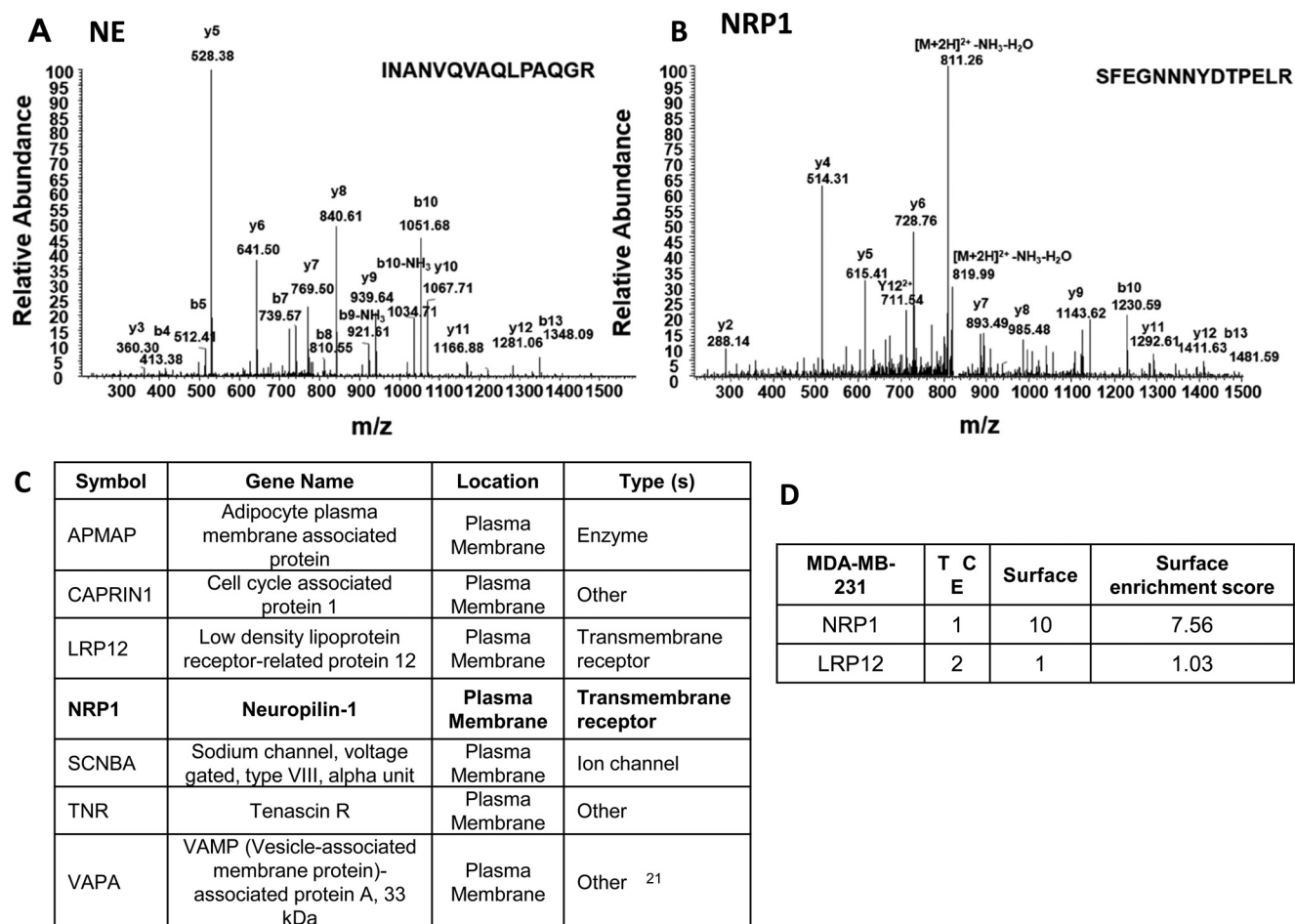


Figure 2. Mass spectra of the immunoprecipitated NE and binding partner NRP1 on MDA-MB-231 cells. A, MS2 spectrum of the NE assigned peptide (Uniprot P08246, residues 539–552). B, MS2 spectrum of the NRP1 assigned peptide (Uniprot E9PEP6, residues 119–133). C, proteins identified in NE pulldown. D, abundance of NRP1 and LRP12 in the MDA-MB-231 cells evaluated by mass spectrometry. TCE, total cell extract.

in Fig. 1, elafin and PMSF does not abolish the NE uptake (Fig. 1E) or NE binding on cell surface (Fig. 1F). The data suggest the existence of a cell surface receptor that binds to NE and mediates internalization independently of its enzyme activity.

To determine whether NE is internalized by a clathrin- or PI3K-dependent pathway, MDA-MB-231 cells were pretreated with chlorpromazine (CPZ), known to inhibit clathrin-coated pit-mediated endocytosis, or wortmannin, an inhibitor of PI3K-dependent internalization (23). The cells were pulsed for 10 min with 10 μ g/ml NE. As observed with transferrin, NE internalization was significantly inhibited in the presence of CPZ and wortmannin (Fig. 1G). The addition of elafin did not reverse this inhibition. Our results strongly indicate the existence of a rapid receptor-mediated uptake mechanism that results in NE uptake via clathrin pits and independently of its enzyme activity.

Because our results in Fig. 1 indicated the existence of a NE receptor, we decided to identify the unknown receptor without bias. We immunoprecipitated NE-binding surface proteins with an anti-NE Ab on MDA-MB-231 cells, and the captured immunoprecipitation was analyzed using nano-HPLC LC-MS/MS (24). As shown in Fig. 2 (A and B), the tryptic peptide from NE and the binding partner NRP1 were clearly identified on the mass spectra of the NE cross-linked complex. Among the seven

cell surface proteins identified by mass spectra, only NRP1 and LRP12 were transmembrane receptors (Fig. 2C). Using the protein database generated after global surface protein biotinylation followed by LC-MS to identify and quantify proteins expressed on cell surface (24), we found NRP1 to be an enriched surface protein in MDA-MB-231 cells, whereas LRP12 was less abundant (Fig. 2D). Furthermore, no difference between LRP12 expression on the surface and total cell extract was observed (Fig. 2D). Notably, NRP1 is also expressed on dendritic cells (25), which have the ability to cross-present soluble antigens including NE (26).

Specificity of NE binding to NRP1

First, to confirm the direct binding of NE to NRP1, we coated microtiter wells with human recombinant NRP_(Phe22–644) and used ELISA to determine the specificity of binding of soluble NE. As shown in Fig. 3A, NE bound to NRP1 in a dose-dependent manner but not to the negative control ovalbumin (OVA). The affinity of NE binding to the NRP1 was measured by bio-layer interferometry with a calculated K_d of 38.7 nM (Fig. 3B). NRP1 has previously been described as an isoform-specific VEGF-165 receptor (27), and thus VEGF-165 was used as a positive control. We found that both NE and the VEGF-165 bound human NRP1, whereas no binding of ovalbumin was

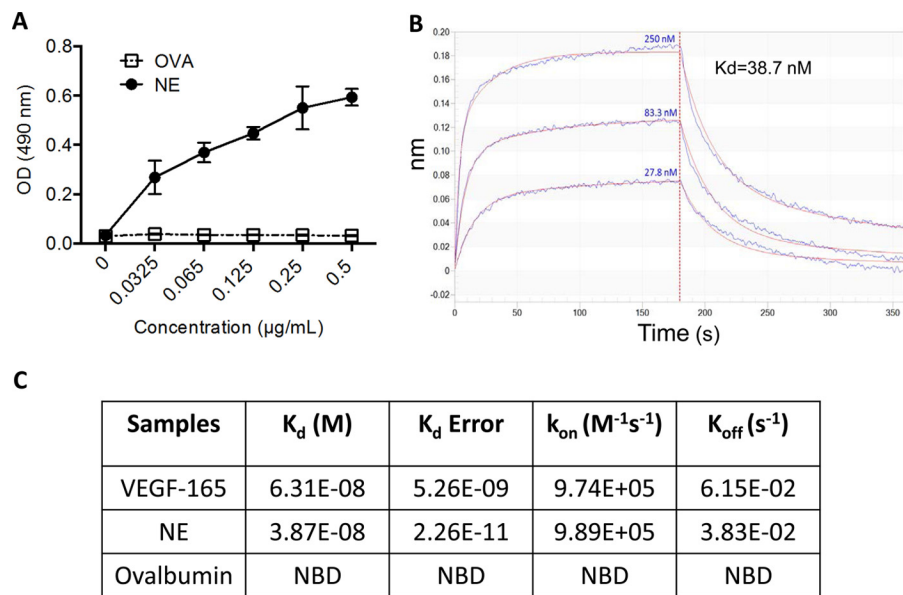


Figure 3. Binding kinetics of NE to NRP1. A, dose-dependent binding of NE to immobilized recombinant human NRP-1 by ELISA. OVA was used to evaluate for nonspecific binding. The results were expressed as the mean of absorbance value obtained from one representative experiment of three, performed in triplicate. B, affinity of NE binding to the NRP1 measured by bio-layer interferometry. NE binds to NRP1-Fc captured on anti-hlgG Fc biosensor with calculated $K_d = 38.7$ nM. Measured response units are in blue. Red lines show results from a 2:1 global fitting interaction model that was used to calculate K_d . C, NRP1 binding constants to ligands. NBD, no binding detected.

detected. As expected, we found that NRP1 binds to VEGF-165 at a K_d value within a double-digit nanomolar range (63.1 nM), indicative of a strong interaction with NRP1 (Fig. 3C). Interestingly, NE with a K_d of 38.7 nM demonstrated a stronger interaction with NRP1 than VEGF-165 (Fig. 3C). Taken together, our data demonstrate that NE is a specific and high-affinity ligand for NRP1.

Various peptides that expose the consensus sequence (R/K/X)X(R/K) at the C terminus (C-end rule) were shown to bind to NRP1 and to internalize in the cells (28). More precisely, a systematic study on mutation of this sequence demonstrated that RRAR, RDAR, RPDR, RPRR, and RPPR are able to bind NRP1 (29). To validate NE binding, we first check the presence of such a motif inside the X-ray structures of NE (PDB entry 3Q76) by using Swiss PDB viewer software. X-ray crystallography indicated that a consensus sequence RRAR (in blue) is contained within an extracellular β -strand of NE protein (Fig. 4A). To characterize and validate the domain of NE interactions with NRP1, ligand-binding assays by ELISA were carried out using two peptides: NE_(130–50R) RRAR motif and another sequence that corresponds to an intracellular β -strand, NE_(F199–220R) (in pink, Fig. 4A). As shown on Fig. 4B, the presumed peptide, NE_(130–50R), binds to His-NRP1_(F22–644K), whereas NE_(F99–220R) does not. To investigate the differences of interaction between different analogs and His-NRP1_(F22–644K), we use some alanine substitutions replacing Arg at position 34 (R34A), 35 (R35A), 37 (R37A), and the triple mutant R34A,R35A,R37A (Fig. 4C). We also test the effect of the replacement of the Ala in position 36 by another inert amino acid Gly (A36G) on NRP1 binding (Fig. 4C). Single substitutions R34A, R35A, and R37A or combined (R34A,R35A,R37A) significantly decrease the binding of the peptide to NRP1 (Fig. 4D), whereas the Ala substitution with Gly (A36G) was not sufficient to abolish the binding to NRP1

(Fig. 4D). These results indicate that NE is able to bind specifically to NRP1 via the consensus sequence RRXR.

NE binds NRP1 on the surface of the MDA-MB-231 cells, and subsequently, this binding is followed by NRP1 internalization

To investigate whether NE binds specifically to NRP1 on the cell surface, we used the CRISPR-cas9 system to knock out NRP1 in MDA-MB-231 cell line (Fig. 5A). The validation of NRP1 knockdown in MDA-MB-231 by CRISPR-Cas9 is presented as supplemental Fig. S2 and supplemental Methods. The absence of NRP1 on the surface of the cells appears to be sufficient to abolish NE surface staining after 10 min of treatment with soluble NE at 4 °C (Fig. 5, B and C).

We used Amnis Image Stream to investigate whether NE induces NRP1 internalization. As shown in Fig. 5D, supplemental Fig. S4, and supplemental Methods, NRP1 was localized on the cell surface and then internalized in the cytosol after 10 min of incubation with soluble NE. To quantify the localization of NRP1, the internalization score was calculated as the ratio of the amount of intracellular fluorescence versus the total amount of fluorescence. The results clearly demonstrated that NRP1 signal was intracellular after NE treatment (Fig. 5E). We concluded that NE treatment induced efficient internalization of NRP1 in MDA-MB-231 cells.

NRP1 mediates NE uptake on various breast cancer cell lines

To determine its role in NE uptake, we transfected the MDA-MB-231 cells with siRNA or shRNA against NRP1. The loss of NRP1 expression was confirmed by Western blot (Fig. 6, A, B, D, and E). The absence of NRP1 expression resulted in a significant decrease in NE uptake in MDA-MB-231 cells (~50% versus si-control or sh-control) (Fig. 6, A and B). Furthermore, we incubated MDA-MB-231 cells with anti-NRP1 antibody prior

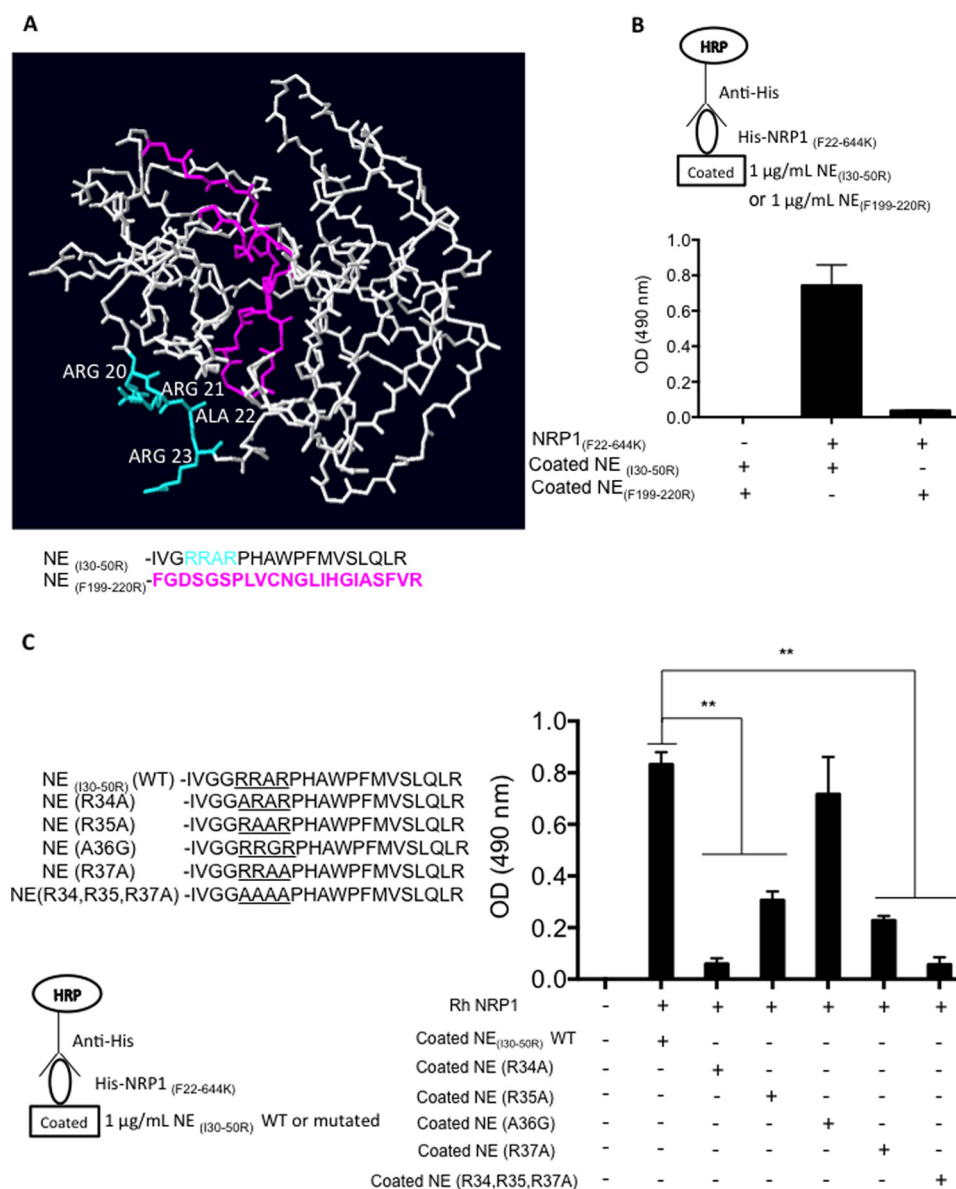


Figure 4. NRP1 interacts with the RRXR motif of NE protein. A, model of neuropilin elastase obtained from electron microscopy (PDB entry 3Q76) was downloaded from the PDB. Selected peptides, NE_(130-50R) and NE_(F199-220R), were docked on the model and visualized using Swiss PDB viewer. In blue is shown RRAR motif contained in NE_(130-50R), and in pink is shown the negative peptide control NE_(F199-220R) used for this study. B, binding of the recombinant human NRP-1, His-NRP1_(F22-644K), to immobilized NE peptide NE_(130-50R) by ELISA. NE_(130-50R) peptide contains the RRAR motif. NE_(F199-220R) was used to evaluate for nonspecific binding. The results were expressed as the mean of absorbance value obtained from three experiments in triplicate. C, binding of recombinant human NRP-1 to the immobilized RRAR sequence (NE_(130-50R)) and its analogs. The results were expressed as the mean of absorbance value obtained from one representative experiment of three, realized in triplicate.

to incubating with NE and found significantly decreased NE uptake (~60% versus isotype control) (Fig. 6C). A similar effect was also seen in Hs 578T BrCa line treated with siRNA against NRP1 (Fig. 6D). Conversely, overexpression of NRP1 in the T47D BrCa line that lacks endogenous NRP1 resulted in a significant increase in NE uptake (3.4-fold increase in MFI versus pCMV-control) (Fig. 6E). Although we showed that NRP1 was implicated in NE uptake in various BrCa cell lines, we could not compare the variation in NE uptake between the cell lines. Indeed, the variability observed between the different cell lines, especially between the T47D and MDA-MB-231 cell lines, is explained by the fact that we performed in-house fluorophore conjugations of anti-NE antibody. These reactions often give variable conjugation efficiencies that could account for vari-

able MFI. In summary, our results demonstrate that NRP1 mediates NE uptake in various breast cancer cell lines.

NRP1 is necessary for breast cancer cell susceptibility to specific lysis by PR1-CTL

We previously showed that the NE-derived peptide PR1 is cross-presented on MDA-MB-231 cells after NE uptake, leading to specific cell lysis by immunotherapies that target PR1/HLA-A2, including PR1-specific CTLs and 8F4 Ab (10, 18). In light of this, we sought to determine the role NRP1-mediated uptake of NE in the cross-presentation of PR1. Cytotoxicity assays showed that NE-treated MDA-MB-231 cells were susceptible to killing by PR1-CTLs generated from various healthy

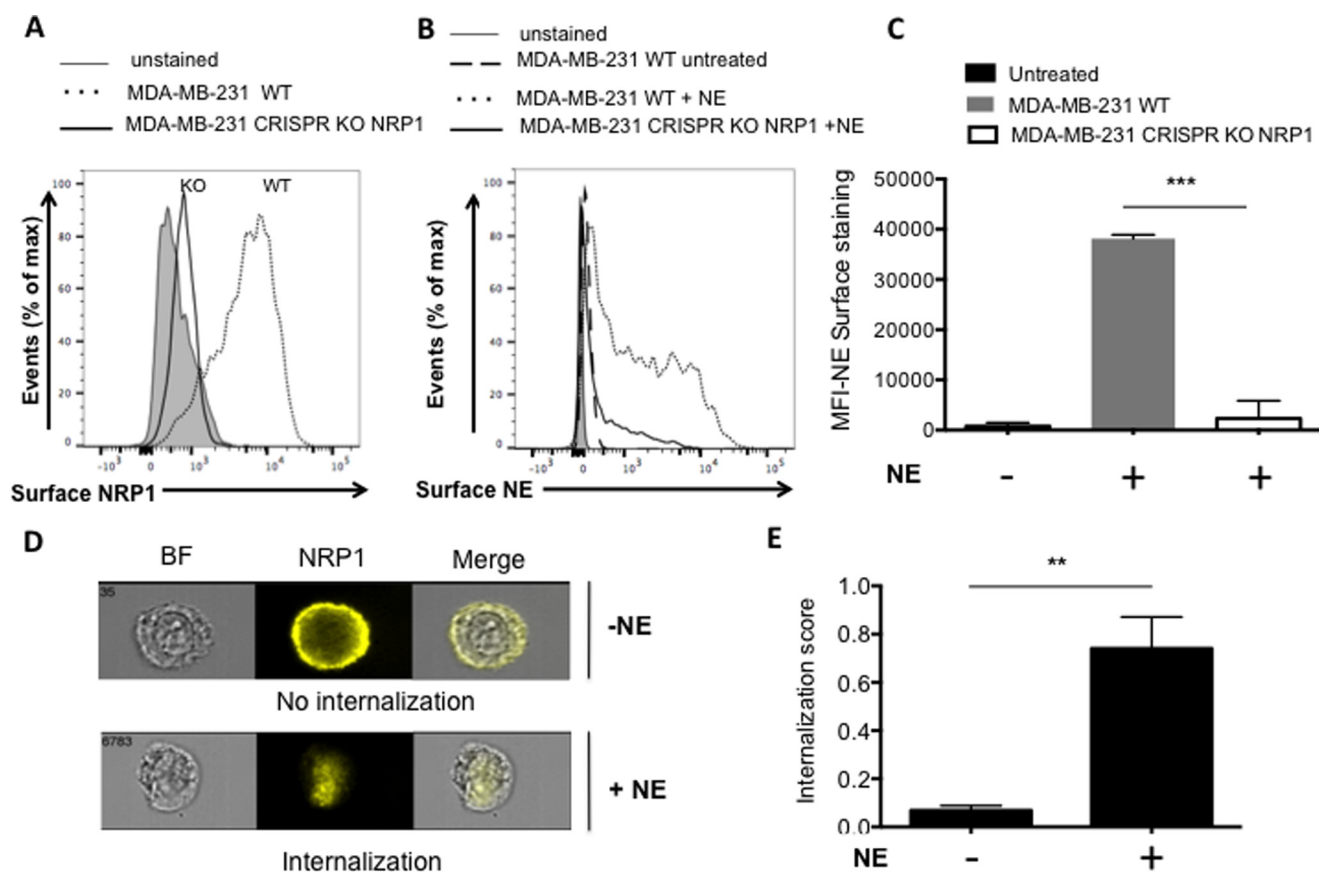


Figure 5. NE binds to NRP1 on MDA-MB-231 cell surface, which internalizes NRP1 after NE binding. A, lack of NRP1 surface expression on MDA-MB-231 human cell lines expressing CRISPR KO NRP1. B and C, NE binds to NRP1 on MDA-MB-231 cells surface. MDA-MB-231 (WT or transfected with CRISPR KO NRP1) cells were pulsed 10 min with NE (10 μ g/ml) and stained with an anti-NE Ab (NP-57) at 4 °C. The representative histogram (B) and data summary (C) of three independent experiments represent the MFI \pm S.E. ***, $p < 0.005$. D and E, determination of NRP1 internalization induced by NE in MDA-MB-231 cells by imaging flow cytometry. D, representative images captured by the Amnis Image Stream X flow cytometer of MDA-MB-231 cells treated with NE 10 μ g/ml for 10 min at 37 °C. The first column shows brightfield (BF) images of the cells, the second column shows images of fluorescence of NRP1, and the third column shows fluorescence merged with the brightfield images of the cells (BF/NRP1). E, internalization score calculated by Amnis IDEAS software: distribution of internalization score of at least 500 cells treated for 10 min at 37 °C. **, $p < 0.01$. The data correspond to the mean values of internalization score \pm S.D. of three independent experiments.

donors (Fig. 7, A and B), confirming our previous observations (10). However, MDA-MB-231 cells lacking NRP1 were not lysed by PR1-CTL derived from the same donor, suggesting that NRP1 is implicated in cross-presentation in MDA-MB-231 cells (Fig. 7, A and B). Our results clearly demonstrate that NRP1 is involved in NE uptake and cross-presentation by BrCa, which is necessary for the specific lysis by PR1-CTL.

Discussion

In this report, we have shown that NRP1 mediates NE uptake by BrCa. More interestingly, we identified NRP1 as an endocytic receptor that transports soluble NE into MDA-MB-231 cells by immunoprecipitation and LC-MS. Direct binding of NE to NRP1 was confirmed by ELISA and bio-layer interferometry. More precisely, we demonstrated that NE interacts with NRP1 through the RRAR sequence contains in its N terminus. Utilizing interfering RNA and the CRISPR-cas9 system, we showed that NRP1 is a receptor for NE binding and uptake on various BrCa cell lines. Moreover, we demonstrated that PR1 cross-presentation by BrCa and cell lysis by PR1-CTL are dependent on NRP1.

Our published data showed that NE is co-localized with EEA-1 following uptake by BrCa cell lines and subsequently

traffics in the endosomes (12). We showed that NE internalization is temperature-sensitive and is significantly decreased in presence of drugs known to inhibit receptors internalization such as PI3K and wortmannin (23) (Fig. 1). In this study, we identified NRP1 as a NE receptor (Fig. 2). NRP1 is known to act as a co-receptor for numerous extracellular ligands and receptors, such as SEMA3A/4A (30) and growth factor receptors VEGF-165 (31) and transforming growth factor- β 1 (32). Interestingly, we showed that NE binds to NRP1 with a similar affinity ($K_d = 38$ nM) to its natural ligand VEGF-165 ($K_d = 63$ nM) (Fig. 3, B and C). The binding observed for NE in our study accounts for the physiological binding and is supported by published reports showing NE blood concentrations up to 1 μ M during inflammatory states (11, 33, 34). It has also been proven that VEGF-165 interacts through the motif CRCDKPRR in its C terminus (27, 35). Recent studies revealed that a consensus sequence (R/K)XX(R/K), found in the C-terminal region of different peptides, is required for binding to NRP1 and internalization (28). By analyzing the crystallography structure (Fig. 4A), we found that NE has a unique RRAR sequence that might explain its ability to bind to NRP1. To validate this sequence, we performed alanine substitution of each residue of the peptide (Fig. 4C). We found that the Arg in positions

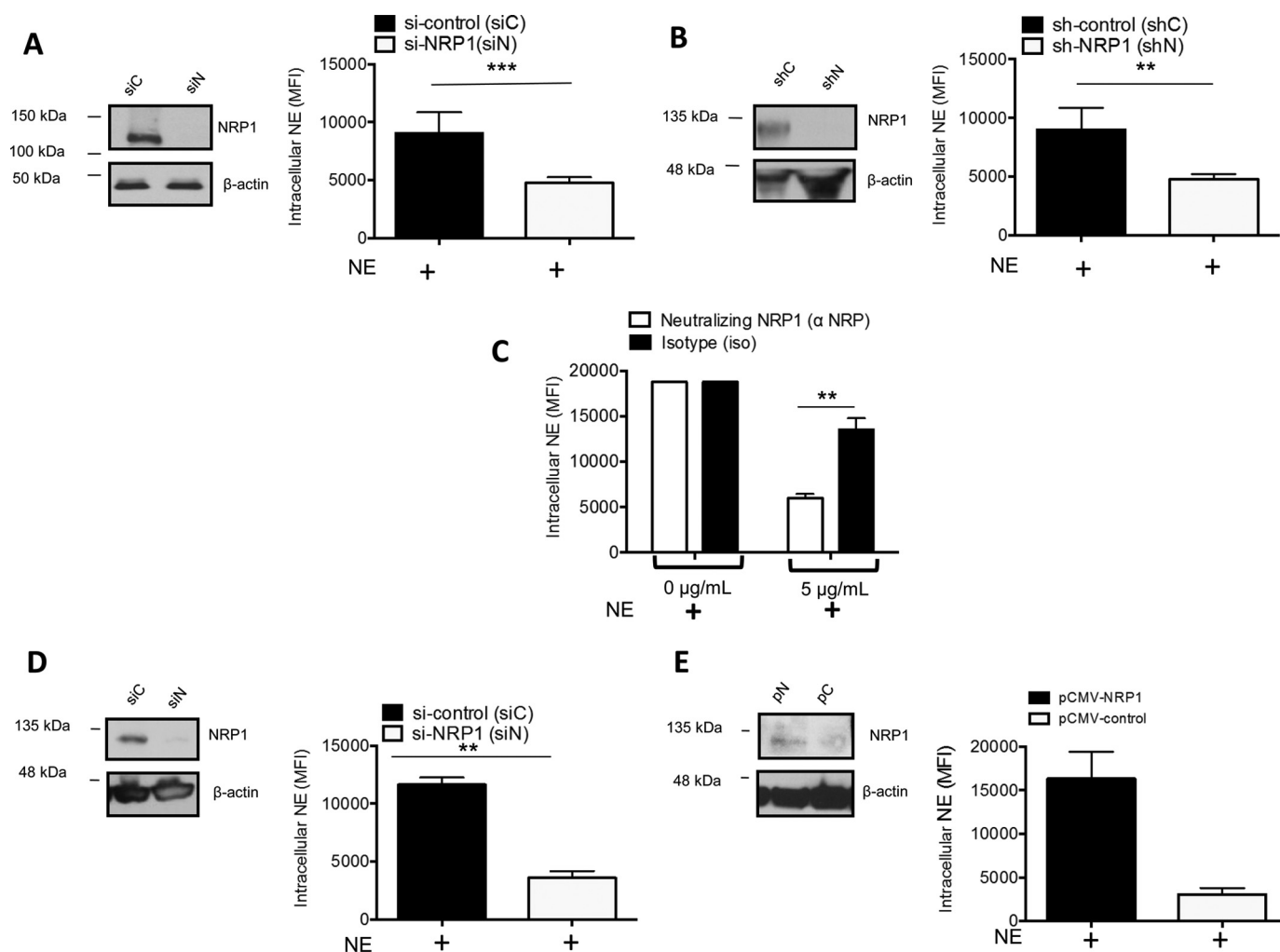


Figure 6. NRP1 mediates NE uptake in BrCa lines. A and B, NRP1 knockdown with siRNA (A) or shRNA (B) decreased NE uptake in MDA-MB-231. C, anti-NRP1 antibody inhibits NE uptake by MDA-MB-231. D and E, validation of NRP1 as a receptor for NE uptake in various BrCa cell lines, by knocking down and overexpressing NRP1 in Hs 578T (D) and T47D (E) BrCa lines, respectively. Intracellular NE was determined by flow cytometry following incubation at 10 μ g/ml for 10 min for all experiments. Graphs display the MFI \pm S.E. representing three individual experiments. **, $p < 0.01$; ***, $p < 0.005$; ****, $p < 0.0001$. Efficiency of transfection was evaluated by immunoblotting. All the immunoblots presented in the figure are cropped.

34, 35, and 37 are essential for NE binding to NRP1 (Fig. 4C). These data are in agreement with the results of Zanuy *et al.* (29), which demonstrated that a RRAR mutant presents high affinity for the b1 domain of NRP1. However, the RRXR is contained in an internal loop and not in the C-terminal region of NE, and the RRXR motif is followed by a proline that can potentially create an unfavorable conformation for the binding to NRP1. We therefore compared the binding of the C-terminal peptide from VEGF-165 (VEGF-165_(R170–191R)), NE peptide_(I30–50R), and intact NE at equimolar concentrations (supplemental Fig. S3 and supplemental Methods). We demonstrated that the intact NE and NE peptide_(I30–50R) bind similarly to NRP1 (supplemental Fig. S3C). Surprisingly, we found that the NE peptide_(I30–50R) binds NRP1 with higher avidity than VEGF-165_(R170–191R) (supplemental Fig. S3, A and B).

Our laboratory previously reported that NE-derived peptide PR1 is cross-presented on MDA-MB-231 cells after NE uptake, leading to their susceptibility to killing by PR1-CTL (10). In this study, we demonstrated that NRP1 silencing in MDA-MB-231

cells was sufficient to suppress PR1 cross-presentation and subsequent killing by PR1-CTL. Furthermore, whereas NE treatment in MDA-MB-231 WT was able to increase the PR1/HLA-A2 presentation on the cell surface as detected by the 8F4 Ab, the knockdown of NRP1 by si-NRP1 or CRISPR KO NRP1 significantly decreased the cross-presentation of PR1/HLA-A2 to a level similar to that seen in the untreated controls (data not shown). These data suggest that NRP1 is required for PR1/HLA-A2 cross-presentation by NE. Nevertheless, NE uptake was not completely abrogated in MDA-MB-231 cells after NRP1 knockdown, suggesting that another receptor may also be capable of internalization (Fig. 5, A–D). These data indicate that NRP1, although likely not the sole receptor for NE uptake, does play a critical role in the uptake of NE and subsequent antigen processing necessary for cross-presentation (Fig. 7, A and B). In contrast to NRP1-mediated internalization, which we have shown to correlate with uptake and cross-presentation, this alternate uptake pathway could potentially be involved in NE-related proliferative effects, as described in numerous studies (2, 3, 11, 36).

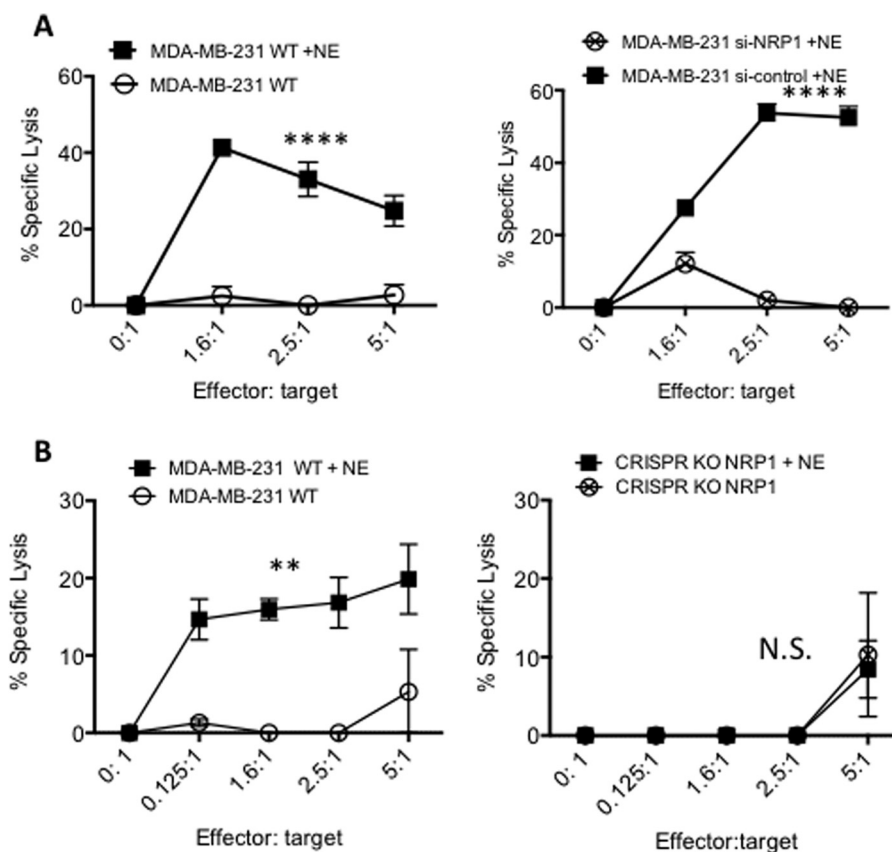


Figure 7. NRP1 mediates specific lysis of MDA-MB-231 cells by PR1-CTL. A and B, MDA-MB-231 cells transfected with si-NRP1 (A) or the CRISPR KO NRP1 (B) were pulsed with NE for 24 h and then incubated with PR1-CTL for specific lysis measured by the calcein-AM cytotoxicity assay. The results are representative of three independent experiments carried out in triplicate. % specific lysis = $(1 - (E_{\text{Experimental}} - E_{\text{Media}}) / (E_{\text{Control}} - E_{\text{Media}})) \times 100$, in which E is fluorescence emission and control group is targets alone. The data are the means \pm S.E. from duplicate wells from a representative experiment. ****, $p < 0.0001$, compared with MDA-MB-231 nontransfected.

Recent work provides evidence that tumor-associated neutrophils are prognosticators, especially in breast and lung tumors (37). By calculating the Pearson's correlation coefficients from individual patient-derived samples using the TCGA database, we demonstrated a moderate to strong positive relationship between CD16, a cell-surface marker of neutrophils that we used as a surrogate marker for NE, and NRP1 mRNA expression in different tumor types (data not shown). Although there is a preponderance of data that link inflammation, tumor-associated neutrophils, and NRP1 with poor outcomes in cancer (9, 38, 39), our published data (10) along with our observations here point to NRP1 as a potential molecule that could be targeted to favorably alter the tumor microenvironment and the innate immune system to generate an effective anti-tumor immune response.

Furthermore, several studies demonstrated that NRP1 is overexpressed in solid tumors compared with normal samples (40–44), indicating NRP1 as a potential therapeutic target. Clinical studies of patients also showed significant correlation between NRP1 expression and clinical staging.

Experimental procedures

Cell culture

MDA-MB-231, Hs 578T, and T47D cells were obtained from American Type Culture Collection (Manassas, VA). All cell

lines were cultured in Dulbecco's modified Eagle's medium/F-12 or in RPMI 1640, supplemented with 10% fetal bovine serum (v/v) (Sigma-Aldrich), 100 units/ml penicillin, and 100 μ g/mg streptomycin (Sigma-Aldrich) and maintained in 5% CO₂ at 37 °C. Cell lines were authenticated by short tandem repeat methodology at the Characterized Cell Line Core Facility at MDACC. Healthy donor apheresis samples were obtained from Gulf Coast Regional Blood Center and MDACC Blood Bank. Peripheral blood mononuclear cells were isolated using standard Histopaque 1077 gradient centrifugation (Sigma-Aldrich).

Peptides and proteins

The human recombinant His-NRP1_(F22-K644) was purchased from R&D System. Purified human NE and elafin were obtained from Athens Research and Technology and Enzo Life Sciences, respectively. Peptides have been synthesized by biosynthesis. The peptide contained the RRAR motif: IVGGRRARPHAWP-FMVSLQLR is referred as NE_(130–50R) (WT). The effects of substitutions were studied by using five purified peptides: Arg-34 \rightarrow Ala (R34A); Arg-35 \rightarrow Ala (R35A); Arg-37 \rightarrow Ala (R37A); the triple substitutions Arg-34 \rightarrow Ala, Arg 35 \rightarrow Ala, and Arg-37 \rightarrow Ala (R34A,R35A,R37A); and the substitution of Ala-36 \rightarrow Gly (A36G), another chemically inert amino acid. The internal sequence FGDSGSPLVCNGLIHGIASFVR, referred to as

NE_(F199–220R) was used as a control. Peptide purity was analyzed by RP-HPLC and was estimated at more than 98%, according to the manufacturer.

Immunoprecipitation of cell surface receptor for NE

MDA-MB-231 cells (1×10^8) were treated with 80 μg of NE (Athens Research and Technology) for 30 min at 4 °C and then incubated with a cross-linker according to the manufacturer's instructions (Pierce Protein Biology by Thermo Scientific). The cells were washed and lysed in nondenaturing lysis buffer (20 mM Tris base, pH 7.5, 150 mM NaCl, 5 mM EDTA, 1% CHAPS, 20 mM iodoacetamide, and 0.2 mM PMSF) for 1 h at 4 °C. Insoluble material was removed by centrifugation at 13,200 rpm for 10 min. Lysates (1.5 mg) were incubated overnight at 4 °C with protein A/G-agarose that had been preincubated with anti-NE antibody (clone NP-57, sc-53388; Santa Cruz Biotechnology) or mouse IgG1 isotype. The immune complexes were washed four times with ice-cold PBS. Immunoprecipitates were eluted with 2 \times Laemmli buffer (120 mM Tris-Cl, pH 6.8, and 4% SDS) and boiled at 100 °C for 10 min. Eluted fractions were desalted using GL-Tip SDB (GL Sciences, CA). Samples were reduced in 15 mM Tris (2-carboxyethyl) phosphine hydrochloride, alkylated with acrylamide (7:1 ratio), and treated with trypsin before being subjected to mass spectrometry analysis.

Mass spectrometry analysis

Tryptic peptides were analyzed by an Orbitrap ELITE MS (Thermo Scientific) coupled to an EASY-nLC 1000 nanoflow chromatography system (Thermo Scientific). The LC separation was performed in a 25-cm, 75- μm -inner-diameter column packed with 3 μm C18 resin (Column Technology Inc.) using a 100-min B pump linear gradient from 5–50% in 300 nl/min, where mobile phase A (0.1% formic acid in 2% acetonitrile) and mobile phase B (0.1% formic acid in 98% acetonitrile) were used. The mass spectrometry was used with MS1 spectrum resolution of 60,000, automatic gain control target of 1×10^6 , and maximum injection time of 150 min. The top 20 precursors were selected for MS2 analysis. MS2 was done by collision-induced dissociation fragmentation with automatic gain control of 3×10^4 , maximum injection time of 10 min, normalized collision energy of 35, isolation width of 2.0 m/z , activation q value of 0.25, and activation time of 10 min. The LC-MS/MS data were processed through Proteome Discoverer version 1.4 (Thermo Scientific) using Sequest HT search engine and Uniprot 1308 database with a false discovery rate of less than 5%, estimated by Target Decoy PSM Validator. The search parameters included Cys alkylated with propionamide (71.03711@C) as a fixed modification and Met oxidation (15.99491@M) as a variable modification. Semi-tryptic search with a maximum of two missed cleavage sites was allowed, and precursor mass tolerance of 10 ppm and fragment mass tolerance of 0.5 Da were applied.

ELISA

For the evaluation of the binding of NE to NRP1, 96-well Maxisorb Immunoplates (Nunc) were coated with human recombinant NRP1 (His-NRP1_(Phe22–644)) (0.5 $\mu\text{g}/\text{ml}$; R&D Systems), blocked with buffer containing 1% w/v BSA in PBS, and incubated for 1 h with a serial dilution (2-fold) of NE (1

$\mu\text{g}/\text{ml}$) or OVA at 37 °C. The plates were then washed and incubated with anti-NE antibody (NP-57) or ovalbumin antibody for 30 min at room temperature. Bound antibodies were detected by incubation with horseradish peroxidase-conjugated goat anti-mouse antibodies (1:2000; Jackson Immuno-Research Laboratories) followed by 3,3',5,5'-tetramethylbenzidine substrate (Becton Dickinson). Parallel ELISA with EndoGrade OVA (Hyglos) was used as the negative control to demonstrate the specificity of NE binding to recombinant NRP1. For characterizing the motif contained in NE that binds NRP1, 1 $\mu\text{g}/\text{ml}$ of NE_(Iso30–50) (WT) and its analogs were coated and blocked with 1% w/v BSA in PBS. His-NRP1_(Phe22–644) (0.5 $\mu\text{g}/\text{ml}$; R&D Systems) was added to each well and incubated for 1 h. The same experiment was realized on a plate coated with BSA to subtract the unspecific binding. After washing the plate, the bound NRP1 was detected with an antibody HRP-conjugated His antibody (Life Technologies). Signal was developed with 3,3',5,5'-tetramethylbenzidine (TMB), and the optical density determined at 450 nm.

Flow cytometry and confocal microscopy

For surface staining, the cells were incubated with NE in 1% BSA in PBS at the indicated times, temperature, and concentrations of NE (Athens Research and Technology). Internalization studies were performed in serum-free RPMI 1640. Inhibition studies were performed with cells that had been preincubated for 1 h at 37 °C with different concentrations (from 0 to 5 $\mu\text{g}/\text{ml}$) of anti-NRP1 antibody (AF 3870; R&D Systems) or isotype control (sc-2717; Santa Cruz Biotechnology). Surface staining was performed for 30 min on ice with anti-NE antibody (clone NP-57, sc-53388; Santa Cruz Biotechnology) directly conjugated to AlexaFluor-647 or anti-NRP1 antibody followed by phosphatidylethanolamine-conjugated secondary antibody (sc-3751; Santa Cruz Biotechnology). For intracellular staining, the cells were permeabilized in perm/wash buffer (BD Biosciences) prior to antibody staining. The data were acquired using a BD LSR Fortessa flow cytometer and were analyzed using FlowJo software (Tree Star, Ashland, OR).

For NRP1 internalization, the cells were analyzed using Amnis ImageStream® Mark II Imaging Flow Cytometer (EMD Millipore Corporation) with 40 \times objective. The results were analyzed by IDEAS image analysis software. A mask representing the whole cell was defined by the bright-field image, and an internal mask was defined by eroding the whole cell mask by 9 pixels, which were eroded to measure only the internalized part. The values of the internalization score were calculated for at least 500 cells/experimental condition. Confocal imaging was performed using a Leica Microsystems SP2 SE confocal microscope (Buffalo Grove) with 63 \times /1.4 oil objective. Leica LCS software (version 2.61) was used for image analysis.

Transfection of plasmids, shRNA, CRISPR KO, and siRNAi against NRP1

BrCa cell lines were transfected with the appropriate plasmids (full-length cDNA encoding NRP1 (pCMV-NRP1) and pCMV-control (pCMV6-XL5) (Origene Technologies)) or siRNA (si-NRP1, sc-36038; si-control A, sc-37007; Santa Cruz Biotechnology) using Amaxa Nucleofector Technology in

accordance with the manufacturer's protocol. The transfection efficiency was confirmed by Western blot analysis of NRP1 48 h after transfection. The cells transduced with lentiviruses (neuropilin shRNA lentiviral particles, sc-36038-V; control shRNA lentiviral particles-A, sc-108080-V; Santa Cruz Biotechnology) were selected in 2 μ g/ml puromycin (Sigma-Aldrich) for 3 weeks. The MDA-MB-231 KO CRISPR NRP1 was generated using the CRISPR-cas9 system based somatic knock-out technology at the Gene Editing/Cellular Model Core Facility from MDACC.

Western blotting

Whole-cell lysates were generated after lysis in radioimmune precipitation assay buffer (Cell Signaling Technology) containing protease inhibitors (Perkin-Elmer). Lysates were separated on 10% SDS-PAGE gels (Bio-Rad) and transferred onto polyvinylidene difluoride membranes (Millipore). After blocking, membranes were probed with anti-NRP1 (clone C-19, sc-7239; Santa Cruz Biotechnology) or anti- β -actin (clone C-4; Merck Millipore). The blots were washed and incubated with anti-goat (sc-2352; Santa Cruz Biotechnology) or anti-mouse horseradish peroxidase-conjugated antibody, respectively (catalog no. 7076S; Cell Signaling Technology). Chemiluminescence (Thermo Fisher Scientific) was captured on Kodak film.

Biolayer interferometry by ForteBio Octet RED384

Biolayer interferometry experiments for binding kinetics were performed on a ForteBio Octet RED384 instrument using anti-human Fc capture (18-5060) biosensor (Pall Fortebio). NRP1-Fc (NR1-H5252; ACRO Biosystems) as a ligand was loaded to the anti-human Fc capture biosensor. Following a baseline incubation in 10 \times kinetics buffer (10 mM phosphate, 150 mM NaCl, 0.02% Tween 20, 0.05% sodium azide, 1 mg/ml BSA, pH 7.4), the loaded biosensors were exposed to a series of analyte concentrations for VEGF165 (VE5-H5248; ACROBiosystems), NE (Athens Research and Technology) and OVA (VWR International) for an association step. Dissociation was monitored in 10 \times kinetics buffer, and background subtraction was used to correct for sensor drifting. All experiments were performed with shaking at 1,000 rpm at 30 $^{\circ}$ C. ForteBio data analysis software was used to fit the data to a 1:1 binding model to extract association and dissociation rates. The K_d was calculated using the ratio k_{off}/k_{on} .

CTL assay

Peripheral blood mononuclear cells from healthy HLA-A2⁺ donors were isolated and stimulated with PR1 peptide (Biosynthesis Inc.) *in vitro*, and calcein-AM cytotoxicity assays were performed as previously described (5, 9). Briefly, 1000 target cells were labeled with 10 μ g/ml calcein-AM (Invitrogen) for 15 min at 37 $^{\circ}$ C. The cells were washed and co-cultured with PR1-CTL (effector cells) at indicated effector:target ratios in a 60-well Terasaki plate. After 4 h of incubation, trypan blue was added, and fluorescence was measured using a Cytation 3 imaging reader (Biotek, Winooski, VT).

Statistical analysis

Comparisons between groups were carried out using Student's *t* test and one-way analysis of variance with the

Tukey's multiple comparison test. The *p* value of 0.05 was set as the criterion for significance. The analyses were performed using Prism 6.0 software.

Author contributions—C. K. was responsible for conception and design, acquisition and analysis of data, and writing the article; S. C. T., H. K., and S. M. H. were responsible for acquisition of data and analysis and interpretation of data content; P. S., K. E. R., K. C.-D., A. V. P., A. A. P., N. Q., D. Z., J. M. M., and C. T. were responsible for development of methodology; A. S., S. L., K. C.-D., and H. L. P. were responsible for conception and design; G. A., L. S. S. J., S. L., E. A. M., A. C. H., and Q. M. were responsible for analysis and interpretation of data and revising the paper; J. J. M. was responsible for study supervision, conception and design, analysis and interpretation of data, and final approval of the paper.

Acknowledgments—We thank Drs. Isere Kuitse and Richard J. Jones (Department of Lymphoma/Myeloma, MDACC); Laura Bover (Department of Genomic Medicine, MDACC); Haven R. Garber, Dan Li, and Annalea Elwell (stem cell transplantation-transplant immunology, MDACC); and Gabriel E. Arias Berrios for technical help. We are grateful to Anne Sutton (Department of Scientific Publications, MDACC) and Andrew H. Wayland (stem cell transplantation-transplant immunology, MDACC) for editing the manuscript.

References

- Korkmaz, B., Horwitz, M. S., Jenne, D. E., and Gauthier, F. (2010) Neutrophil elastase, proteinase 3, and cathepsin G as therapeutic targets in human diseases. *Pharmacol. Rev.* **62**, 726–759
- Gregory, A. D., Hale, P., Perlmutter, D. H., and Houghton, A. M. (2012) Clathrin pit-mediated endocytosis of neutrophil elastase and cathepsin G by cancer cells. *J. Biol. Chem.* **287**, 35341–35350
- Nawa, M., Osada, S., Morimitsu, K., Nonaka, K., Futamura, M., Kawaguchi, Y., and Yoshida, K. (2012) Growth effect of neutrophil elastase on breast cancer: favorable action of sivelestat and application to anti-HER2 therapy. *Anticancer Res.* **32**, 13–19
- Sun, Z., and Yang, P. (2004) Role of imbalance between neutrophil elastase and α 1-antitrypsin in cancer development and progression. *Lancet Oncol.* **5**, 182–190
- Bagheri-Yarmand, R., Biernacka, A., Hunt, K. K., and Keyomarsi, K. (2010) Low molecular weight cyclin E overexpression shortens mitosis, leading to chromosome missegregation and centrosome amplification. *Cancer Res.* **70**, 5074–5084
- Porter, D. C., Zhang, N., Danes, C., McGahren, M. J., Harwell, R. M., Faruki, S., and Keyomarsi, K. (2001) Tumor-specific proteolytic processing of cyclin E generates hyperactive lower-molecular-weight forms. *Mol. Cell. Biol.* **21**, 6254–6269
- Sato, N., Sutani, A., Oya, H., Yamaguchi, T., Saito, K., Kobayashi, K., Nagata, M., Hagiwara, K., and Kanazawa, M. (2007) [Prognostic significance of neutrophil elastase inhibitor in patients with acute lung injury and interstitial pneumonia]. *Nihon Kokyuki Gakkai Zasshi* **45**, 237–242
- Yamashita, J., Akizuki, M., Jotsuka, T., Harao, M., and Nakano, S. (2006) Neutrophil elastase predicts trastuzumab responsiveness in metastatic breast cancer. *Breast J.* **12**, 288
- Akizuki, M., Fukutomi, T., Takasugi, M., Takahashi, S., Sato, T., Harao, M., Mizumoto, T., and Yamashita, J. (2007) Prognostic significance of immunoreactive neutrophil elastase in human breast cancer: long-term follow-up results in 313 patients. *Neoplasia* **9**, 260–264
- Alatrash, G., Mittendorf, E. A., Sergeeva, A., Sukhumalchandra, P., Qiao, N., Zhang, M., St John, L. S., Ruisaard, K., Haugen, C. E., Al-Atrache, Z., Jakher, H., Philips, A. V., Ding, X., Chen, J. Q., Wu, Y., et al. (2012) Broad cross-presentation of the hematopoietically derived PR1 antigen on solid tumors leads to susceptibility to PR1-targeted immunotherapy. *J. Immunol.* **189**, 5476–5484

11. Houghton, A. M., Rzymkiewicz, D. M., Ji, H., Gregory, A. D., Egea, E. E., Metz, H. E., Stolz, D. B., Land, S. R., Marconcini, L. A., Kliment, C. R., Jenkins, K. M., Beaulieu, K. A., Mouded, M., Frank, S. J., Wong, K. K., *et al.* (2010) Neutrophil elastase-mediated degradation of IRS-1 accelerates lung tumor growth. *Nat. Med.* **16**, 219–223
12. Mittendorf, E. A., Alatrash, G., Qiao, N., Wu, Y., Sukhumalchandra, P., St John, L. S., Philips, A. V., Xiao, H., Zhang, M., Ruisaard, K., Clise-Dwyer, K., Lu, S., and Molldrem, J. J. (2012) Breast cancer cell uptake of the inflammatory mediator neutrophil elastase triggers an anticancer adaptive immune response. *Cancer Res.* **72**, 3153–3162
13. Metz, H. E., and Houghton, A. M. (2011) Insulin receptor substrate regulation of phosphoinositide 3-kinase. *Clin. Cancer Res.* **17**, 206–211
14. Molldrem, J. J., Lee, P. P., Wang, C., Felio, K., Kantarjian, H. M., Champlin, R. E., and Davis, M. M. (2000) Evidence that specific T lymphocytes may participate in the elimination of chronic myelogenous leukemia. *Nat. Med.* **6**, 1018–1023
15. Qazilbash, M. H., Wieder, E., Thall, P. F., Wang, X., Rios, R., Lu, S., Kano-dia, S., Ruisaard, K. E., Giralt, S. A., Estey, E. H., Cortes, J., Komanduri, K. V., Clise-Dwyer, K., Alatrash, G., Ma, Q., Champlin, R. E., *et al.* (2017) PR1 peptide vaccine induces specific immunity with clinical responses in myeloid malignancies. *Leukemia* **31**, 697–704
16. Rezvani, K., Yong, A. S., Mielke, S., Jafarpour, B., Savani, B. N., Le, R. Q., Eniafe, R., Musse, L., Boss, C., Kurlander, R., and Barrett, A. J. (2011) Repeated PR1 and WT1 peptide vaccination in Montanide-adjuvant fails to induce sustained high-avidity, epitope-specific CD8⁺ T cells in myeloid malignancies. *Haematologica* **96**, 432–440
17. Ma, Q., Garber, H. R., Lu, S., He, H., Tallis, E., Ding, X., Sergeeva, A., Wood, M. S., Dotti, G., Salvado, B., Ruisaard, K., Clise-Dwyer, K., John, L. S., Rezvani, K., Alatrash, G., *et al.* (2016) A novel TCR-like CAR with specificity for PR1/HLA-A2 effectively targets myeloid leukemia in vitro when expressed in human adult peripheral blood and cord blood T cells. *Cytotherapy* **18**, 985–994
18. Sergeeva, A., Alatrash, G., He, H., Ruisaard, K., Lu, S., Wygant, J., McIntyre, B. W., Ma, Q., Li, D., St John, L., Clise-Dwyer, K., and Molldrem, J. J. (2011) An anti-PR1/HLA-A2 T-cell receptor-like antibody mediates complement-dependent cytotoxicity against acute myeloid leukemia progenitor cells. *Blood* **117**, 4262–4272
19. Sergeeva, A., He, H., Ruisaard, K., St John, L., Alatrash, G., Clise-Dwyer, K., Li, D., Patenia, R., Hong, R., Sukhumalchandra, P., You, M. J., Gagea, M., Ma, Q., and Molldrem, J. J. (2016) Activity of 8F4, a T-cell receptor-like anti-PR1/HLA-A2 antibody, against primary human AML *in vivo*. *Leukemia* **30**, 1475–1484
20. McGowan, S. E., Arbeit, R. D., Stone, P. J., and Snider, G. L. (1983) A comparison of the binding and fate of internalized neutrophil elastase in human monocytes and alveolar macrophages. *Am. Rev. Respir. Dis.* **128**, 688–694
21. Campbell, E. J. (1982) Human leukocyte elastase, cathepsin G, and lactoferrin: family of neutrophil granule glycoproteins that bind to an alveolar macrophage receptor. *Proc. Natl. Acad. Sci. U.S.A.* **79**, 6941–6945
22. Chaudhary, B., Khaled, Y. S., Ammori, B. J., and Elkord, E. (2014) Neuropilin 1: function and therapeutic potential in cancer. *Cancer Immunol. Immunother.* **63**, 81–99
23. Mukherjee, S., Ghosh, R. N., and Maxfield, F. R. (1997) Endocytosis. *Endocytosis Physiol. Rev.* **77**, 759–803
24. Taguchi, K., Fukusaki, E., and Bamba, T. (2014) Supercritical fluid chromatography/mass spectrometry in metabolite analysis. *Bioanalysis* **6**, 1679–1689
25. Tordjman, R., Lepelletier, Y., Lemarchandel, V., Cambot, M., Gaulard, P., Hermine, O., and Roméo, P. H. (2002) A neuronal receptor, neuropilin-1, is essential for the initiation of the primary immune response. *Nat. Immunol.* **3**, 477–482
26. Alatrash, G., Ono, Y., Sergeeva, A., Sukhumalchandra, P., Zhang, M., St John, L. S., Yang, T. H., Ruisaard, K., Armistead, P. M., Mittendorf, E. A., He, H., Qiao, N., Rodriguez-Cruz, T., Liang, S., Clise-Dwyer, K., *et al.* (2012) The role of antigen cross-presentation from leukemia blasts on immunity to the leukemia-associated antigen PR1. *J. Immunother.* **35**, 309–320
27. Soker, S., Takashima, S., Miao, H. Q., Neufeld, G., and Klagsbrun, M. (1998) Neuropilin-1 is expressed by endothelial and tumor cells as an isoform-specific receptor for vascular endothelial growth factor. *Cell* **92**, 735–745
28. Teesalu, T., Sugahara, K. N., Kotamraju, V. R., and Ruoslahti, E. (2009) C-end rule peptides mediate neuropilin-1-dependent cell, vascular, and tissue penetration. *Proc. Natl. Acad. Sci. U.S.A.* **106**, 16157–16162
29. Zanuy, D., Kotla, R., Nussinov, R., Teesalu, T., Sugahara, K. N., Alemán, C., and Haspel, N. (2013) Sequence dependence of C-end rule peptides in binding and activation of neuropilin-1 receptor. *J. Struct. Biol.* **182**, 78–86
30. Janssen, B. J., Malinauskas, T., Weir, G. A., Cader, M. Z., Siebold, C., and Jones, E. Y. (2012) Neuropilins lock secreted semaphorins onto plexins in a ternary signaling complex. *Nat. Struct. Mol. Biol.* **19**, 1293–1299
31. Djordjevic, S., and Driscoll, P. C. (2013) Targeting VEGF signalling via the neuropilin co-receptor. *Drug Discov. Today* **18**, 447–455
32. Glinka, Y., Stoilova, S., Mohammed, N., and Prud'homme, G. J. (2011) Neuropilin-1 exerts co-receptor function for TGF- β -1 on the membrane of cancer cells and enhances responses to both latent and active TGF- β . *Carcinogenesis* **32**, 613–621
33. Henriksen, P. A. (2014) The potential of neutrophil elastase inhibitors as anti-inflammatory therapies. *Curr. Opin Hematol.* **21**, 23–28
34. Zhao, P., Lieu, T., Barlow, N., Sostegni, S., Haerteis, S., Korbacher, C., Liedtke, W., Jimenez-Vargas, N. N., Vanner, S. J., and Bunnett, N. W. (2015) Neutrophil elastase activates protease-activated receptor-2 (PAR2) and transient receptor potential vanilloid 4 (TRPV4) to cause inflammation and pain. *J. Biol. Chem.* **290**, 13875–13887
35. Jia, H., Bagherzadeh, A., Hartzoulakis, B., Jarvis, A., Löhr, M., Shaikh, S., Aqil, R., Cheng, L., Tickner, M., Esposito, D., Harris, R., Driscoll, P. C., Selwood, D. L., and Zachary, I. C. (2006) Characterization of a bicyclic peptide neuropilin-1 (NP-1) antagonist (EG3287) reveals importance of vascular endothelial growth factor exon 8 for NP-1 binding and role of NP-1 in KDR signaling. *J. Biol. Chem.* **281**, 13493–13502
36. Hattar, K., Franz, K., Ludwig, M., Sibelius, U., Wilhelm, J., Lohmeyer, J., Savai, R., Subtil, F. S., Dahlem, G., Eul, B., Seeger, W., Grimminger, F., and Grandel, U. (2014) Interactions between neutrophils and non-small cell lung cancer cells: enhancement of tumor proliferation and inflammatory mediator synthesis. *Cancer Immunol. Immunother.* **63**, 1297–1306
37. Gentles, A. J., Newman, A. M., Liu, C. L., Bratman, S. V., Feng, W., Kim, D., Nair, V. S., Xu, Y., Khuong, A., Hoang, C. D., Diehn, M., West, R. B., Plevritis, S. K., and Alizadeh, A. A. (2015) The prognostic landscape of genes and infiltrating immune cells across human cancers. *Nature medicine* **21**, 938–945
38. Grandclement, C., and Borg, C. (2011) Neuropilins: a new target for cancer therapy. *Cancers* **3**, 1899–1928
39. Jensen, T. O., Schmidt, H., Möller, H. J., Donskov, F., Høyer, M., Sjoegren, P., Christensen, I. J., and Steiniche, T. (2012) Intratumoral neutrophils and plasmacytoid dendritic cells indicate poor prognosis and are associated with pSTAT3 expression in AJCC stage I/II melanoma. *Cancer* **118**, 2476–2485
40. Cheng, W., Fu, D., Wei, Z. F., Xu, F., Xu, X. F., Liu, Y. H., Ge, J. P., Tian, F., Han, C. H., Zhang, Z. Y., and Zhou, L. M. (2014) NRP-1 expression in bladder cancer and its implications for tumor progression. *Tumour Biol.* **35**, 6089–6094
41. Ghosh, S., Sullivan, C. A., Zerkowski, M. P., Molinaro, A. M., Rimm, D. L., Camp, R. L., and Chung, G. G. (2008) High levels of vascular endothelial growth factor and its receptors (VEGFR-1, VEGFR-2, neuropilin-1) are associated with worse outcome in breast cancer. *Hum. Pathol.* **39**, 1835–1843
42. Latil, A., Bièche, I., Pesche, S., Valéri, A., Fournier, G., Cussenot, O., and Lidereau, R. (2000) VEGF overexpression in clinically localized prostate tumors and neuropilin-1 overexpression in metastatic forms. *Int. J. Cancer* **89**, 167–171
43. Li, L., Jiang, X., Zhang, Q., Dong, X., Gao, Y., He, Y., Qiao, H., Xie, F., Xie, X., and Sun, X. (2016) Neuropilin-1 is associated with clinicopathology of gastric cancer and contributes to cell proliferation and migration as multifunctional co-receptors. *J. Exp. Clin. Cancer Res.* **35**, 16
44. Stephenson, J. M., Banerjee, S., Saxena, N. K., Cherian, R., and Banerjee, S. K. (2002) Neuropilin-1 is differentially expressed in myoepithelial cells and vascular smooth muscle cells in preneoplastic and neoplastic human breast: a possible marker for the progression of breast cancer. *Int. J. Cancer* **101**, 409–414

Neuropilin-1 mediates neutrophil elastase uptake and cross-presentation in breast cancer cells

Celine Kerros, Satyendra C. Tripathi, Dongxing Zha, Jennifer M. Mehrens, Anna Sergeeva, Anne V. Philips, Na Qiao, Haley L. Peters, Hiroyuki Katayama, Pariya Sukhumalchandra, Kathryn E. Ruisaard, Alexander A. Perakis, Lisa S. St. John, Sijie Lu, Elizabeth A. Mittendorf, Karen Clise-Dwyer, Amanda C. Herrmann, Gheath Alatrash, Carlo Toniatti, Samir M. Hanash, Qing Ma and Jeffrey J. Molldrem

J. Biol. Chem. 2017, 292:10295-10305.

doi: 10.1074/jbc.M116.773051 originally published online May 3, 2017

Access the most updated version of this article at doi: [10.1074/jbc.M116.773051](https://doi.org/10.1074/jbc.M116.773051)

Alerts:

- [When this article is cited](#)
- [When a correction for this article is posted](#)

[Click here](#) to choose from all of JBC's e-mail alerts

Supplemental material:

<http://www.jbc.org/content/suppl/2017/05/03/M116.773051.DC1>

This article cites 44 references, 14 of which can be accessed free at

<http://www.jbc.org/content/292/24/10295.full.html#ref-list-1>